

R.M. - 1897

1111.1

27

Library. L.M.G.L.

Copy

TECHNICAL MEMORANDUMS

NATIONAL ADVISORY COMMITTEE FOR AERONAUTICS

No. 723

AN AIRFOIL SPANNING AN OPEN JET

By J. Stüber

Ingenieur-Archiv, Vol. III, 1932

Washington
September 1933



3 1176 01437 3857

NATIONAL ADVISORY COMMITTEE FOR AERONAUTICS

TECHNICAL MEMORANDUM NO. 723

AN AIRFOIL SPANNING AN OPEN JET*

By J. Stüber

SUMMARY

The first part of the report treats of the theory involved. Proceeding from the fundamental problem on the mutual relation of a wing and free boundaries the distribution of the circulation is determined for an airfoil spanning an open jet of rectangular section at different aspect ratios, and then for an open jet of circular section.

The solution is obtained by means of a Fourier series and computations have been performed for different values of the variables.

The second part describes the experiments performed for the purpose of proving the theory. The results confirm the theory. In conclusion it defines the induced drag of a wing extending across an open jet and compares it with the drag of a monoplane having a span equal to the jet width at equal total lift.

I. INTRODUCTION

The present report treats of the case of an airfoil extending across an open jet on the basis of Prandtl's airfoil theory (reference 2).

The problem consists in analyzing the phenomena produced on an airfoil of constant section when extending - normally to the jet axis - through the center of an open jet or rectangular or circular section.

* "Der durch einen Freistrahrl hindurchgesteckte Tragflügel["] (reference 1). Ingenieur-Archiv. vol. III, 1932, pp. 338-355.

In contradistinction to the calculation in the airfoil theory regarding the wing of finite span but in an infinite fluid the wing here is, so to say, of infinite span, whereas the fluid has certain boundaries. A differentiation is made between two kinds of boundaries: fixed walls and open jet boundaries, i.e., such, beyond which the velocity vector disappears. The present problem pertains to the case of free boundaries. Practical interest attaches to the solution of the problem (reference 3). In steam turbine design one employs vanes spanning the jets. Besides, the airfoil extending across an open jet affords an aerodynamic test arrangement of more than usual simplicity (reference 2, p. 52). With circular jet section the solution answers in part the question as to the interference of the slipstream on the wing and the control surfaces of an airplane.

II. Theory

The condition to be fulfilled with the existence of free jet boundaries is the constancy of the pressure on them. The pressure equals that of the fluid at rest.

In the first order the condition is fulfilled by putting the interference velocity-component on the free boundaries in the flow direction equal to zero, this velocity component being due to a disturbance for instance, an airfoil across a jet.

The following coordinate system is used:

x - direction coincident with the wing,

y - direction of flow,

z - downward.

With u, v, w, as velocity components of the interference on the free boundary and V the stream velocity, Bernoulli's theorem gives

$$(V + v)^2 + u^2 + w^2 = \text{const.} = V^2$$

or

$$2Vv + u^2 + v^2 + w^2 = 0$$

In first order this gives the above condition that $v = 0$ on the free boundaries (reference 2). The method of solving such problems is to assume an infinite fluid and to choose the appropriate velocity component in the flow direction equal to zero on the surfaces which are to represent the free boundaries. The changes produced by these additional flows constitute the effect of the free boundaries.

Problem 1: A plane as free boundary. - Assuming that in the half space $x > 0$ the rate of fluid flow is V and static in the $x < 0$ half, then the plane $x = 0$ is a free boundary. A cylindrical wing of infinite span lying on the x axis has the circulation σ at point $x \leq 0$, because the pressure at top and bottom edge of the wing is the same. Accordingly the question is posed as to how the circulation drops from Γ_∞ (infinite fluid) to $\Gamma(x) = \sigma$ when $x = 0$. The solution of this problem gives in simple form information on the behavior of the flow at the point at which the airfoil passes through the free boundary. The singularity established for this point should likewise occur with all other boundary surfaces (circular jet, etc.). The addition of an equal wing portion with angle of attack $-\alpha$ in the negative x axis to the wing portion, with $+\alpha$ angle in positive x axis, produces no interference velocity v in the plane $x = 0$ with assumedly constant air stream in fluid of infinite extent. The angle $-\alpha$ is so defined that with it the wing has the same but opposite circulation as with $+\alpha$. Then at each point of $x = 0$ there is an equal but inversely directed component v of the one wing part conformably to the v component of another part, so that the resultant disappears. On the premises of the first order the v component as well as the w component becomes zero. The u component normal to $x = 0$ effects a deformation of the boundary.

The subsequent treatment of the problem which leads to the question of the circulation distribution of a wing with variable change of angle of attack, is developed in the following problem, in which the above problem is contained as a special case.

Problem 2: Two parallel planes as free boundaries. - Bounded by the surfaces $x = 0$ and $x = l$, the rate of fluid flow is assumed as V . Admittedly, in fluid of infinite extent an airfoil lying on axis x produces no interference velocities v on $x = 0$ and $x = l$ when its angle of attack alternates periodically between $+\alpha$ and $-\alpha$.

The period is equal to $2l$ and the discontinuities occur at $x = 0, \pm l, \pm 2l, \pm 3l, \dots$. The problem of a wing with variable angle of attack change is known in the airfoil theory as the aileron problem (reference 4).

In the treatment of that problem the distribution of the circulation over a wing with a periodic, sudden change of angle of attack has been determined.

Since it was intended to employ the same line of reasoning in a subsequent calculation it may not be amiss to repeat Betz and Petersohn's method in so far as it relates to our subject.

Let Γ_∞ be the circulation about the airfoil in infinite fluid and at angle of attack α^* , and t = the wing chord. Then the circulation at point x is

$$\Gamma(x) = \Gamma_\infty f(x, t, l).$$

The periodically changing angle of attack is expanded in a Fourier series (reference 5):

$$\alpha(x) = \alpha^* \frac{4}{\pi} \sum_0^\infty \frac{\sin(2n+1)\pi \frac{x}{l}}{2n+1}$$

Next we form $\Gamma(x)$ as an analogous Fourier series with as yet unknown coefficients

$$\Gamma(x) = \Gamma_\infty \sum_0^\infty a_{(2n+1)} \sin(2n+1)\pi \frac{x}{l}$$

Then the velocities in z direction produced at the locus of the wing are according to the airfoil theory (reference 2)

$$w(x) = \Gamma_\infty \sum_0^\infty \frac{a_{(2n+1)}}{4l} \frac{(2n+1)\pi}{\sin \pi(2n+1)\frac{x}{l}}$$

Then $\Gamma(x) = \frac{c V t}{2} \left[\alpha(x) - \frac{w(x)}{V} \right]$ with $c = \frac{d c_{\alpha\infty}}{d \alpha_\infty}$

$$\Gamma(x) = \frac{cVta^*}{2} \sum_{n=0}^{\infty} \frac{4 \sin(2n+1)\pi \frac{x}{l}}{\pi(2n+1)} - \Gamma_{\infty} \sum_{n=0}^{\infty} \frac{ct(2n+1)\pi a_{(2n+1)}}{8l} \sin(2n+1)\pi \frac{x}{l}$$

Allowing for

$$\frac{c t V a^*}{2} = \Gamma_{\infty}$$

yields

$$\Gamma(x) = \Gamma_{\infty} \sum_{n=0}^{\infty} \left[\frac{4}{\pi(2n+1)} - \frac{ct(2n+1)\pi a_{(2n+1)}}{8l} \right] \sin(2n+1)\pi \frac{x}{l}$$

Putting

$$\Gamma(x) = \Gamma_{\infty} \sum_{n=0}^{\infty} a_{(2n+1)} \sin(2n+1)\pi \frac{x}{l}$$

we have, since the coefficients of the corresponding terms of the two Fourier series must be equal:

$$a_{(2n+1)} = \frac{4}{\pi(2n+1)[1 + \frac{ct\pi}{8l}(2n+1)]}$$

and consequently

$$\Gamma(x) = \Gamma_{\infty} \frac{4}{\pi} \sum_{n=0}^{\infty} \frac{\sin(2n+1)\pi \frac{x}{l}}{(2n+1) + \frac{ct\pi}{8l}(2n+1)^2}$$

We write $\frac{8l}{ct\pi} = \lambda$, so that

$$\begin{aligned} \frac{\Gamma(x)}{\Gamma_{\infty}} &= \frac{4}{\pi} \sum_{n=0}^{\infty} \frac{\sin(2n+1)\pi \frac{x}{l}}{(2n+1) + \frac{1}{\lambda}(2n+1)^2} \\ &= \frac{4}{\pi} \left[\sum_{n=0}^{\infty} \frac{\sin(2n+1)\pi \frac{x}{l}}{2n+1} - \sum_{n=0}^{\infty} \frac{\sin(2n+1)\pi \frac{x}{l}}{2n+1+\lambda} \right] \\ &= 1 - \frac{4}{\pi} \sum_{n=0}^{\infty} \frac{\sin(2n+1)\pi \frac{x}{l}}{2n+1+\lambda} \quad \text{for } 0 < x < l. \end{aligned}$$

The calculation and representation of the distribution curve is developed with the aid of the solution of the next problem.

Allowing the period $2l$ to grow against ∞ in the present problem, yields problem 1. According to Betz and Petersohn (reference 4. p. 256), it results for this case in

$$\frac{\Gamma(x)}{\Gamma_0} = 1 - \frac{2}{\pi} \sin \frac{8x}{ct} \text{Ci} \frac{8x}{ct} - \cos \frac{8x}{ct} \left(1 - \frac{2}{\pi} \text{Si} \frac{8x}{ct} \right)$$

wherein Si and Ci denote the functions of the integrals \sin and \cos , respectively. (reference 6). It is found that the circulation distribution has a singularity of form $x \lg x$ at the focal point.

Problem 3: Open jet of rectangular section.— The conditions at the boundaries of a rectangular open jet of width l and height h are fulfilled for a wing spanning the jet with the following assumptions. For infinite fluid we find in plane $y = 0$ at the points $z = mh$ (m includes all positive and negative whole numbers as well as zero) infinitely long wings with periodic, variable angle-of-attack change, alternating between $+\alpha^*$ and $-\alpha^*$. The period is equal to $2l$ and the reversals are at points $x = 0, \pm l, \pm 2l, \dots$ (fig. 1). With this assumption all velocity components in the direction of flow on the surfaces $x = ml$ and $z = (2m + 1) \frac{h}{2}$ are made to disappear.

According to the airfoil theory, the w component of the velocity induced at the locus of the wing in the x axis is

$$\begin{aligned} w(x) &= \frac{1}{4\pi} \int_{-\infty}^{+\infty} \sum_{m=-\infty}^{+\infty} \frac{d\Gamma(x_1)}{dx_1} \frac{(x - x_1)}{(x - x_1)^2 + (mh)^2} dx_1 \\ &= \frac{1}{2\pi} \int_{-\infty}^{+\infty} \sum_{m=1}^{\infty} \frac{d\Gamma(x_1)}{dx_1} \frac{\frac{x-x_1}{h}}{\left(\frac{x-x_1}{h}\right)^2 + m^2} \frac{dx_1}{h} + \frac{1}{4\pi} \int_{-\infty}^{+\infty} \frac{d\Gamma(x_1) dx_1}{dx_1 (x-x_1)} \end{aligned}$$

Then (reference 7)

$$\sum_{m=1}^{\infty} \frac{a}{a^2 + m^2} = \frac{\pi}{2} \operatorname{Csch} \pi a - \frac{1}{2a}$$

Consequently,

$$w(x) = \frac{1}{4h} \int_{-\infty}^{+\infty} \frac{d\Gamma(x_1)}{dx_1} \operatorname{Csch} \frac{\pi}{h} (x - x_1) dx_1.$$

The angle of attack can be expanded in a Fourier series:

$$\alpha(x) = \alpha^* \frac{4}{\pi} \sum_{n=0}^{\infty} \frac{\sin(2n+1)\pi \frac{x}{l}}{2n+1}$$

and we form

$$\Gamma(x) = \Gamma_{\infty} \sum_{n=0}^{\infty} a_{(2n+1)} \sin(2n+1)\pi \frac{x}{l}$$

Then

$$w(x) = \Gamma_{\infty} \sum_{n=0}^{\infty} \frac{a_{(2n+1)}(2n+1)\pi}{4h} \int_{-\infty}^{+\infty} \cos(2n+1)\pi \frac{x_1}{l} \operatorname{Csch} \frac{\pi}{h} (x-x_1) dx_1$$

The integral in this equation becomes with $\frac{\pi}{h}(x-x_1) = v$

$$\begin{aligned} J &= \frac{h}{\pi} \cos(2n+1)\pi \frac{x}{l} \int_{-\infty}^{+\infty} \cos(2n+1) \frac{h}{l} v \operatorname{Csch} v dv \\ &\quad + \frac{h}{\pi} \sin(2n+1)\pi \frac{x}{l} \int_{-\infty}^{+\infty} \sin(2n+1) \frac{h}{l} v \operatorname{Csch} v dv \end{aligned}$$

It is

$$\int_{-\infty}^{+\infty} \cos(2n+1) \frac{h}{l} v \operatorname{Csch} v dv = 0$$

and (reference 8)

$$\int_{-\infty}^{+\infty} \sin(2n+1) \frac{h}{l} v \operatorname{Csch} v dv = \pi \frac{e^{(2n+1)\frac{h}{l}\pi} + 1}{e^{(2n+1)\frac{h}{l}\pi} - 1}$$

Thus

$$w(x) \Gamma_{\infty} \sum_{n=0}^{\infty} \frac{a_{(2n+1)}(2n+1)\pi}{4l} \frac{e^{(2n+1)\frac{h}{l}\pi} + 1}{e^{(2n+1)\frac{h}{l}\pi} - 1} \sin(2n+1)\pi \frac{x}{l}$$

The insertion of a Fourier series for $\alpha(x)$ and $w(x)$ in equation

$$\Gamma(x) = \frac{c V t}{2} \left[a(x) - \frac{w(x)}{V} \right]$$

results in

$$a_{(2n+1)} = \frac{4}{\pi(2n+1)} \left[1 + \frac{c \operatorname{t} \pi(2n+1)}{8l} \frac{e^{(2n+1) \frac{h}{l} \pi} + 1}{e^{(2n+1) \frac{h}{l} \pi} - 1} \right]$$

and consequently,

$$\frac{\Gamma(x)}{\Gamma_\infty} = \frac{4}{\pi} \sum_0^\infty \frac{\sin(2n+1) \pi \frac{x}{l}}{(2n+1) \left[1 + \frac{c \operatorname{t} \pi(2n+1)}{8l} \frac{e^{(2n+1) \frac{h}{l} \pi} + 1}{e^{(2n+1) \frac{h}{l} \pi} - 1} \right]}$$

Calculation of function $\Gamma(x)/\Gamma_\infty$ - Permitting h to grow against ∞ in the last equation gives

$$\frac{e^{(2n+1) \frac{h}{l} \pi} + 1}{e^{(2n+1) \frac{h}{l} \pi} - 1} = 1$$

and we obtain with equation

$$\frac{\Gamma(x)}{\Gamma_\infty} = 1 - \frac{4}{\pi} \sum_0^\infty \frac{\sin(2n+1) \pi \frac{x}{l}}{2n + 1 + \lambda}$$

the solution of problem 2 again.

The point, therefore, is to compute

$$S = \sum_0^\infty \frac{\sin(2n+1) \pi \frac{x}{l}}{2n + 1 + \lambda}$$

Assuming x/l to take successively the values 0.5, 0.25, 0.125, 0.0625, we obtain

$$S_1 = \sin \frac{\pi}{2} \sum_0^\infty \frac{(-1)^n}{2n + 1 + \lambda}$$

$$S_2 = \sin \frac{\pi}{4} \left[\sum_0^\infty \frac{(-1)^n}{4n + 1 + \lambda} + \sum_0^\infty \frac{(-1)^n}{4n + 3 + \lambda} \right]$$

$$S_3 = \sin \frac{\pi}{8} \left[\sum_{n=0}^{\infty} \frac{(-1)^n}{8n+1+\lambda} + \sum_{n=0}^{\infty} \frac{(-1)^n}{8n+7+\lambda} \right]$$

$$+ \sin \frac{3\pi}{8} \left[\sum_{n=0}^{\infty} \frac{(-1)^n}{8n+3+\lambda} + \sum_{n=0}^{\infty} \frac{(-1)^n}{8n+5+\lambda} \right]$$

$$S_4 = \sin \frac{\pi}{16} \left[\sum_{n=0}^{\infty} \frac{(-1)^n}{16n+1+\lambda} + \sum_{n=0}^{\infty} \frac{(-1)^n}{16n+15+\lambda} \right]$$

$$+ \sin \frac{3\pi}{16} \left[\sum_{n=0}^{\infty} \frac{(-1)^n}{16n+3+\lambda} + \sum_{n=0}^{\infty} \frac{(-1)^n}{16n+13+\lambda} \right]$$

$$+ \sin \frac{5\pi}{16} \left[\sum_{n=0}^{\infty} \frac{(-1)^n}{16n+5+\lambda} + \sum_{n=0}^{\infty} \frac{(-1)^n}{16n+11+\lambda} \right]$$

$$+ \sin \frac{7\pi}{16} \left[\sum_{n=0}^{\infty} \frac{(-1)^n}{16n+7+\lambda} + \sum_{n=0}^{\infty} \frac{(-1)^n}{16n+9+\lambda} \right].$$

All existent sums are of the type of $S = \sum_{n=0}^{\infty} \frac{(-1)^n}{an+b}$.
Then

$$\sum_{n=0}^{\infty} \frac{(-1)^n}{an+b} = \int^1_0 \frac{t^{b-1}}{1+t^a} dt$$

Partial fractionation of this integral leads to a logarithm and an arc tangent, by means of which the sums can be computed. The calculation was carried through for integral λ values from 1 to 9, which practically covers all interesting ratios of jet width to wing chord. The obtained figures are given in the first part of table I ($\frac{h}{l} = \infty$). Figure 2 shows the trend of $\Gamma(x)/\Gamma_\infty$ for constant wing chord and increasing jet width. The enveloping curve for $\frac{l}{t} = \infty$ is Betz and Petersohn's distribution curve.

In figure 3 the course is given for constant jet width and different wing chords. This solves problem 2. Prescribing definite values (rectangular jet) for h/l , the expression

$$\frac{e^{(2n+1)\frac{h}{l}\pi} + 1}{e^{(2n+1)\frac{h}{l}\pi} - 1} = \epsilon(2n+1, \frac{h}{l}) \text{ is seen to}$$

converge toward 1 after very few terms of the series. Thus the above computed sums can be used by bearing in mind the effect of the function $\epsilon(2n+1, \frac{h}{l})$ on the first terms

of the series. The $\Gamma(x)/\Gamma_\infty$ values are given in table I. The trend of the curves for different jet sections with varying wing chord is shown in figures 4, 5, and 6, whereas figures 7 to 10 give $\Gamma(x)/\Gamma_\infty$ versus λ for different h/l . This solves problem 3.

Problem 4: Open jet of circular section.— A solution can be effected as follows. As shown at the beginning of the report, the fulfillment of the jet condition within the first order stipulates that the component of the interference velocity in direction x becomes zero at the jet boundary. The integration along the streamline reveals that the potential of the interference velocities at the jet boundary must be constant and has the value zero. Consequently, the streamlines of the interference flows are perpendicular to the jet boundary. This condition is fulfilled with the circular jet in a section far aft of the wing. The thus formulated boundary condition prescribes that the disturbance due to the circular contour be confined to radial direction only.

For symmetrical reasons the origin of the coordinates hereinafter is placed in the center of the jet. Within this circle the equation

$$\Gamma(x) = \frac{c V t}{2} \left[\alpha^* - \frac{w(x)}{V} \right]$$

must be fulfilled for constant α^* and t . With conformal transformation the radius of the circle becomes $R = 1$. Then the circle is plotted by the function

$$z = \frac{i - e^{i\zeta}}{1 - ie^{i\zeta}} \quad \text{or} \quad \zeta = -i \lg \frac{i - z}{1 - iz}$$

onto a period strip (fig. 11).

TABLE I

$\frac{h}{l}$	λ	0.5	0.25	$\frac{x}{l} =$	0.125	0.0625
8	1	0.559	0.482		0.361	0.252
	2	0.727	0.654		0.523	0.386
	3	0.805	0.747		0.624	0.478
	4	0.849	0.802		0.689	0.543
	5	0.877	0.835		0.738	0.596
	6	0.897	0.862		0.770	0.636
	7	0.911	0.877		0.800	0.670
	8	0.925	0.893		0.819	0.698
	9	0.930	0.903		0.837	0.722
1.0	1	0.531	0.470		0.352	0.248
	2	0.702	0.634		0.513	0.382
	3	0.784	0.733		0.616	0.474
	4	0.831	0.790		0.682	0.539
	5	0.860	0.823		0.730	0.592
	6	0.883	0.853		0.765	0.633
	7	0.898	0.869		0.795	0.667
	8	0.910	0.885		0.815	0.695
	9	0.920	0.896		0.833	0.720
0.7854 $(= \frac{\pi}{4})$	1	0.498	0.447		0.338	0.242
	2	0.678	0.614		0.502	0.376
	3	0.765	0.717		0.609	0.470
	4	0.813	0.776		0.675	0.536
	5	0.845	0.812		0.724	0.589
	6	0.868	0.837		0.759	0.630
	7	0.886	0.860		0.790	0.665
	8	0.899	0.877		0.810	0.693
	9	0.909	0.888		0.829	0.718

TABLE I (cont'd)

$\frac{h}{l}$	λ		$\frac{x}{l} =$		
		0.5	0.25	0.125	0.0625
0.58905 $(= \frac{3\pi}{16})$	1	0.458	0.419	0.323	0.222
	2	0.632	0.586	0.487	0.368
	3	0.723	0.690	0.594	0.462
	4	0.778	0.752	0.661	0.529
	5	0.815	0.791	0.715	0.583
	6	0.841	0.823	0.752	0.625
	7	0.861	0.841	0.782	0.660
	8	0.876	0.861	0.802	0.688
	9	0.889	0.874	0.821	0.714
0.31831 $(= \frac{1}{\pi})$	1	0.333	0.319	0.261	0.205
	2	0.499	0.477	0.422	0.333
	3	0.600	0.588	0.531	0.430
	4	0.667	0.659	0.605	0.501
	5	0.713	0.705	0.661	0.557
	6	0.750	0.745	0.701	0.600
	7	0.778	0.771	0.734	0.638
	8	0.800	0.795	0.761	0.667
	9	0.819	0.813	0.784	0.694
0.2	1	0.238	0.236	0.211	0.172
	2	0.382	0.379	0.349	0.293
	3	0.481	0.478	0.453	0.387
	4	0.557	0.552	0.531	0.457
	5	0.612	0.609	0.589	0.515
	6	0.653	0.652	0.634	0.561
	7	0.688	0.686	0.672	0.599
	8	0.716	0.715	0.701	0.632
	9	0.739	0.738	0.726	0.660

The x axis ($-1 < x < 1$) becomes the ξ axis ($0 < \xi < \pi$) because $x = \frac{-\cos \xi}{1 + \sin \xi}$. The section of the periphery lying in the semi-plane $x < 0$ becomes the straight line $\xi = 0$, the other half becomes $\xi = \pi$. The above equation must be transformed in the ξ plane.

It is

$$\frac{d \Gamma(x)}{d x} dx = \frac{d \Gamma(\xi)}{d \xi} d \xi$$

$$w(x) dx = w(\xi) d \xi$$

Then

$$\frac{d z}{d \xi} = \frac{-2 i e^{i \xi}}{(1 - i e^{i \xi})^2}$$

$$\frac{d x}{d \xi} = \frac{1}{1 + \sin \xi}$$

Accordingly,

$$\Gamma(\xi) = \frac{c V \xi}{2} [\alpha^* - \frac{w(\xi)}{V} (1 + \sin \xi)]$$

This equation must be fulfilled in the ξ plane. The fulfillment of the jet condition which stipulates in the ξ plane that on both boundary straights $\xi = 0$ and $\xi = \pi$ only flows in direction of the normals may occur, can be effected by reflection method as shown in problem 2. It results in the equation

$$\frac{\Gamma(\xi)}{\Gamma_\infty} \frac{1}{1 + \sin \xi} = \frac{\pm 1}{1 + \sin \xi} - \frac{ct}{2} \frac{w(\xi)}{\Gamma_\infty}$$

the minus sign for the intervals $(2 p - 1)\pi < \xi < 2 p \pi$, the plus sign for the intervals $2 p \pi < \xi < (2 p + 1)\pi$. The solution is again effected by expansion in a Fourier series. We expand

$$\frac{1}{1 + |\sin \xi|} = \sum_0^{\infty} b_{2m} \cos 2m \xi$$

$$\frac{\pm 1}{1 + |\sin \xi|} = \sum_0^{\infty} \beta_{(2n+1)} \sin (2n+1) \xi$$

with

$$b_{2m} = \frac{4}{\pi c} \int_0^{\pi/2} \frac{\cos 2m x}{1 + \sin x} dx$$

$$\beta_{(2n+1)} = \frac{4}{\pi} \int_0^{\pi/2} \frac{\sin (2n+1)x}{1 + \sin x} dx$$

With as yet unknown coefficients

$$\frac{\Gamma(\xi)}{\Gamma_\infty} = \sum_0^{\infty} a_{(2n+1)} \sin (2n+1) \xi$$

we have

$$\frac{w(\xi)}{\Gamma_\infty} = \frac{1}{4} \sum_0^{\infty} a_{(2n+1)} (2n+1) \sin (2n+1) \xi$$

Then we put $\frac{8}{ct} = \lambda$, so that

$$\begin{aligned} & \sum_0^{\infty} a_{(2n+1)} \sin (2n+1) \xi \sum_0^{\infty} b_{2m} \cos 2m \xi \\ &= \sum_0^{\infty} \beta_{(2n+1)} \sin (2n+1) \xi - \frac{1}{\lambda} \sum_0^{\infty} a_{(2n+1)} (2n+1) \sin (2n+1) \xi \end{aligned}$$

and

$$\begin{aligned} & \sum_{n=0}^1 \sum_{m=0}^{\infty} a_{(2n+1)} b_{2m} [\sin(2n+1+2m)\xi + \sin(2n+1-2m)\xi] \\ &= \sum_{n=0}^{\infty} [\beta_{(2n+1)} - \frac{1}{\lambda} a_{(2n+1)} (2n+1)] \sin (2n+1) \xi \end{aligned}$$

The comparison of the coefficients of corresponding terms discloses the following system for the desired coefficients $a_{(2n+1)}$:

$$\begin{aligned}
 a_1(2b_0 + \frac{2}{\lambda}) &= 2\beta_1 - [a_3(b_2 - b_4) + a_5(b_4 - b_6) + a_7(b_6 - b_8) + \dots], \\
 a_3(2b_0 + \frac{2}{\lambda}) &= 2\beta_3 - [a_1(b_2 - b_4) + a_5(b_2 - b_8) + a_7(b_4 - b_{10}) + \dots], \\
 a_5(2b_0 + \frac{2}{\lambda}) &= 2\beta_5 - [a_1(b_4 - b_6) + a_3(b_2 - b_8) + a_7(b_8 - b_{12}) + \dots], \\
 a_7(2b_0 + \frac{2}{\lambda}) &= 2\beta_7 - [a_1(b_6 - b_8) + a_3(b_4 - b_{10}) + a_5(b_2 - b_{12}) + \dots].
 \end{aligned}$$

which is solvable by iteration. The calculation of the integrals

$$J_1 = \int_0^{\pi/2} \frac{\cos 2m\xi}{1 + \sin \xi} d\xi \text{ and } J_2 = \int_0^{\pi/2} \frac{\sin (2n+1)\xi}{1 + \sin \xi} d\xi$$

for defining b_{2m} and $\beta_{(2n+1)}$ gives the values in a form which offers difficulties to further calculation. It is more expedient to approximate the function $f(\xi) = \frac{1}{1 + \sin \xi}$ in the interval $0 \leq \xi \leq \pi$ by a rational function.

A first approximation would form the parabola $y = \frac{2}{\pi^2} (\xi - \frac{\pi}{2})^2 + \frac{1}{2}$, which at point $\xi = 0, \pi/2$ and π coincide with the previous curve. Approximation with function

$$y = a \left(\xi - \frac{\pi}{2} \right)^4 + b \left(\xi - \frac{\pi}{2} \right)^2 + \frac{1}{2}$$

is better, wherein a and b are so defined that at point $\xi = 0$ (for $\xi = \pi$ also for symmetrical reasons) the value of the function and the first derivation agree with the previously cited function. The subsequent calculation is made with this approximation. It is

$$a = \frac{4}{\pi^3} - \frac{8}{\pi^4} \quad b = \frac{4}{\pi^2} - \frac{1}{\pi}$$

hence

$$y = \left(\frac{4}{\pi^2} - \frac{8}{\pi^4} \right) \xi^4 - \left(\frac{8}{\pi^3} - \frac{16}{\pi^4} \right) \xi^3 + \left(\frac{5}{\pi} - \frac{8}{\pi^2} \right) \xi^2 - \xi + 1$$

Accordingly

$$b_{2m} = \frac{4}{\pi} \int_0^{\pi/2} y(\xi) \cos 2m\xi d\xi$$

$$\beta_{(2n+1)} = \frac{4}{\pi} \int_0^{\pi/2} y(\xi) \sin(2n+1)\xi d\xi$$

Now the coefficients $a_{(2n+1)}$ can be defined by means of the above cited system of equations. We computed $\frac{\Gamma(\xi)}{\Gamma_\alpha}$ at the points $\xi = \frac{\pi}{2}, \frac{\pi}{4}, \frac{\pi}{8}$ and $\frac{\pi}{16}$ for integral values of λ from 1 to 9, which, reduced to the z plane give the figures in table II.

TABLE II

$\frac{16}{c t \pi} \frac{R}{R}$	$\frac{x}{R} =$			
	0.0	0.414	0.670	0.821
1	0.519	0.462	0.355	0.224
2	0.692	0.631	0.491	0.356
3	0.774	0.725	0.597	0.447
4	0.821	0.784	0.665	0.510
5	0.853	0.825	0.714	0.570
6	0.877	0.853	0.751	0.616
7	0.891	0.872	0.782	0.651
8	0.906	0.890	0.802	0.680
9	0.915	0.899	0.819	0.709

The trend of the distribution curves is seen in figures 12 and 13.

III. EXPERIMENT

The calculations described in the preceding sections were proved experimentally. The set-up is illustrated in figure 14. At a is the nozzle of a blower. The illustration shows the arrangement for the measurements on the circular jet ($R = 20$ cm). In another case the jet was given a square section ($h = l = 30$ cm), and in still another a rectangular section ($h = 15$ cm, $l = 30$ cm, hence $\frac{h}{l} = 0.5$ cm). The velocity distribution across the jet section proved to be sufficiently constant in all cases. A model airfoil (Göttingen No. 398) of $t = 10$ cm chord was mounted on a U-shaped frame h. The distance from the nozzle edge to the leading edge of the wing was 10 cm, because the static pressure assumes a constant value at that distance. The wing has at b 16 orifices distributed across the section (figure 15). The test stations are connected to the multiple pressure gauge c by means of tubes and rubber hose. The pressure patterns were photographed with camera d, as illustrated in figure 16. The wing can be made to slide normally to the jet axis with the frame h (fig. 14) along the guide rail g. The amount of displacement is determined on scale f and marked at every exposure. The measurements included - with rectangular jet section - the following angles of attack: -3° , 0° , 3° , 6° , 9° ; and - with circular jet section: -2° , 0° , 3° , and 5° . The wind speed was 30 m/s. The figures taken from the pressure photographs were made nondimensional by division with the dynamic pressure of the undisturbed flow q. By plotting the figures against the orifices projected on the air stream direction as abscissa we obtain pressure profiles whose contents represent the lift quota of the test section. Several examples for the square jet are shown in figures 17 to 19. The figure above each pressure profile indicates the ratio of distance of the test section from the jet center to half the jet width. With $c_a(x) = \frac{dA}{qt dx}$ the pertinent $c_a(x)$ is obtained for each test section.

IV. THEORY vs. TEST

Analysis of profile constant c. - According to the profile measurements (reference 9)

$$c_a = 3.82 \alpha^*$$

for the employed airfoil (α^* measured in radians from point $c_a = 0$). These measurements had been made with a characteristic value $E = 6,000 \text{ mm} \times \text{m/s}$, in contradistinction to our measurements with $E = 3,000 \text{ mm} \times \text{m/s}$. Allowing for this fact results in

$$c_a = 3.66 \alpha^*$$

as probable value according to Wieselsberger's experiments (reference 9, p. 54, etc.)

The equation is valid for $\frac{l}{t} = 5$ aspect ratio. For conversion to the wing of infinite span we used Glauert's formula (reference 10) for wings with rectangular contour. It yields

$$c_{a\infty} = 5.02 \alpha^*_{\infty} \quad \text{and} \quad \frac{d c_{a\infty}}{d \alpha_{\infty}} = c = 5.02$$

Determination of actual jet dimensions.— In order to study the effect of the jet contraction and the mixing zone at the jet boundary on the jet dimensions the course of the flow velocity was measured in the plane of the wing leading edge normally to the jet axis. The constant value within the jet served as height of a rectangle; its width, so proportioned that rectangle and velocity profile are of equal volume, is defined as actual jet width. Thus:

$h = l = 29.1 \text{ cm}$ for the square jet,

$h = 14.6 \text{ cm}$, $l = 29.1 \text{ cm}$ for the rectangular jet.

The jet radius for the circular jet was ascertained as equal to the nozzle radius ($R = 20 \text{ cm}$), because of the opposition offered by a special design of the nozzle (constriction before the mouth) against the otherwise produced contraction.

The wing chord was $t = 10 \text{ cm}$; thus

$$\lambda = \frac{8l}{ct\pi}$$

yields

$$\lambda = 1.47$$

for the square and rectangular jet

and

$$\lambda_k = 2.02$$

for the circular jet.

Comparison.- The values for $\frac{\Gamma(x)}{\Gamma_\infty}$ can be read from the computed tables and from figures 7 to 10.

It is

$$c_a(x) = \frac{d A(x)}{\frac{\rho}{2} v^2 t d x} \quad (\rho = \text{fluid density})$$

and with

$$\frac{d A(x)}{d x} = \rho v \Gamma(x)$$

it is

$$c_a(x) = \frac{2 \Gamma(x)}{v t}$$

similarly

$$c_{a\infty} = \frac{2 \Gamma_\infty}{v t}$$

thus

$$c_a(x) = c_{a\infty} \frac{\Gamma(x)}{\Gamma_\infty}$$

as used for computing the theoretical values of $c_a(x)$ for the different angles of attack. The trend of the lift distribution with square jet section is shown in figure 20, with rectangular section in figure 21, and with circular section in figure 22. The small circles denote the measured values. The trend of the theoretical and of the experimental curves is patently in fairly close accord, the measured values being somewhat less than the theoretical. This discrepancy diminishes as the angles of attack decreases. The cause of the greater discrepancy toward the jet boundary with the angular jet sections is that the blower jet has rounded-off corners as a result of the mixing zone. With the circular jet where this effect does not exist, the agreement is therefore substantially closer. The very close accord of the total lift as defined by theory and test is noteworthy.

Calculation of drag.- According to the airfoil theory (reference 2, p. 27)

$$d W = \rho \Gamma(x) w(x) d x$$

which, when supplemented by

$$w(x) = v \left(\alpha - \frac{2 \Gamma(x)}{c v t} \right)$$

or with $\frac{c}{2} v t \alpha = \Gamma_\infty$

$$w(x) = \frac{c}{2} v^2 t \alpha^2 \frac{1 - \frac{\Gamma(x)}{\Gamma_\infty}}{\Gamma_\infty}$$

yields (reference 11)

$$dW = c \frac{\rho}{2} v^2 t \alpha^2 \frac{\Gamma(x)}{\Gamma_\infty} \left(1 - \frac{\Gamma(x)}{\Gamma_\infty} \right) dx$$

The form of the function $\frac{\Gamma(x)}{\Gamma_\infty} \left(1 - \frac{\Gamma(x)}{\Gamma_\infty} \right)$, that is, the distribution of the drag density is illustrated in figures 23 to 27 for different jet sections with varying wing chord.

In conclusion we compare the drag of a wing extending across an open jet with the drag of an identical wing (span equals jet width) for infinite fluid width an assumedly elliptical lift distribution, the total lift to be the same. It is

$$dA(x) = \rho \Gamma(x) V dx$$

and with $\frac{c}{2} v t \alpha = \Gamma_\infty$, it becomes

$$dA(x) = c \frac{\rho}{2} v^2 t \alpha \frac{\Gamma(x)}{\Gamma_\infty} dx$$

Likewise

$$A = c \frac{\rho}{2} v^2 t \alpha \int_l^0 \frac{\Gamma(x)}{\Gamma_\infty} dx$$

We put

$$\int_l^0 \frac{\Gamma(x)}{\Gamma_\infty} dx = \kappa l$$

thus

$$A = c \frac{\rho}{2} v^2 t \alpha \kappa l$$

Consequently

$$c \frac{\rho}{2} V^2 t \alpha^2 = \frac{A^2}{c \frac{\rho}{2} V^2 t \kappa^2 l^2}$$

and

$$W = \frac{A^2}{c \frac{\rho}{2} V^2 t \kappa^2 l^2} \int_0^l \frac{\Gamma(x)}{\Gamma_\infty} \left(1 - \frac{\Gamma(x)}{\Gamma_\infty}\right) dx$$

Then we substitute β for $\frac{l}{t}$, write the theoretical value of 2π in place of c ($= \frac{d c \alpha_\infty}{d \alpha_\infty}$), and put

$$\int_0^l \frac{\Gamma(x)}{\Gamma_\infty} \left(1 - \frac{\Gamma(x)}{\Gamma_\infty}\right) dx = \gamma l$$

so that

$$W = \frac{2 A^2}{\pi \rho V^2 l^2} \frac{\beta \gamma}{2 \kappa^2}$$

The factor $\frac{2 A^2}{\pi \rho V^2 l^2}$ is the drag of an airfoil of span l in infinite fluid and with assumedly elliptical distribution of lift (reference 2, p. 32).

The factor $\eta = \frac{\beta \gamma}{2 \kappa^2}$ indicates how many times the drag of a wing spanning an open jet is greater than the compared monoplane of span equal to jet width in a fluid of infinite extent. The value of κ can be obtained by planimetry of figures 3 to 6 and the value of γ from figures 23 to 27. The dependence of η on t/l is consequently so slight as to be within accuracy of the calculation.

For the rectangular jet section we have

$$\frac{h}{l} = \infty \quad 1.0 \quad 0.318 \quad 0.2$$

$$\eta = 1.50 \quad 1.67 \quad 3.10 \quad 4.52$$

The curve is shown in figure 28. For the circular jet it disclosed $\eta = 1.84$, and for the wing of minimum drag with given lift extending across a circular jet,

proper warping of the wing being permitted, $\eta = 1.74$ according to K. Pohlhausen (reference 2, p. 56).

Translation by J. Vanier,
National Advisory Committee
for Aeronautics.

REFERENCES

1. Göttinger Dissertation. Referent: Prof. Dr. L. Prandtl.
2. Prandtl, L.: Tragflügeltheorie. Neudruck in Prandtl-betz, Vier Abhandlungen zur Hydrodynamik und Aerodynamik, p. 9, etc., Göttingen 1927. N.A.C.A. T.M. Nos. 9 and 10, 1920, (abridged).
3. Ackeret, J.: Energieverluste an Gleichdruckturbinen Stodolafestschrift, Zürich, 1929, p. 1.
Ackeret, J.: In "Hydraulische Probleme," Berlin, 1926, p. 177.
4. Betz, A. and Petersohn, E.: Contribution to the Aileron Theory. T.M. No. 542, N.A.C.A., 1929.
5. Knopp, K.: Theorie der unendlichen Reihen, 1924, p. 375.
6. Jahnke, E. and Emde, F.: Funktionentafeln, Liepzig, 1923, p. 19.
7. Schlömilch, O.: Arch. d. Math. Phys. 1849, Part 12, p. 130.
8. de Haan, D. Bierens: Tables d'intégrales définies, Leiden 1867, p. 388.
9. Prandtl, L.: Ergebnisse der Aerodynamischen Versuchsanstalt zu Göttingen, vol. 1, pp. 92 and 106. Munich, 1921,
10. Glauert, H. and Holl, H.: Grundlagen der Tragflügel-theorie, Berlin 1929, p. 132.
11. Trefftz, E.: Z.f.a.M.M., vol. 1, 1921, p. 206.

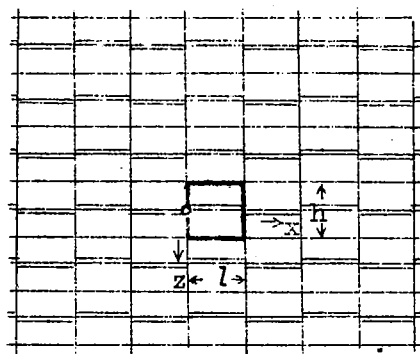


Figure 1.-Reflection method for
rectangular jct section.

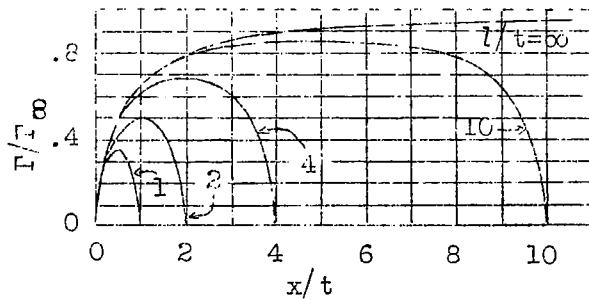


Figure 2.-Circulation distribution with two
parallel planes as jet boundary
versus width of jet.

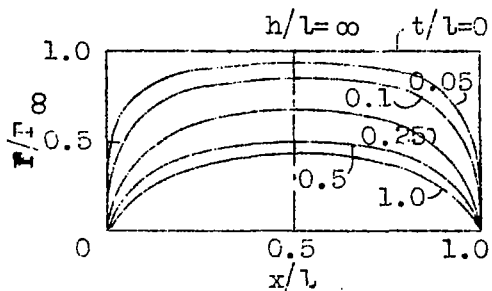


Figure 3.-Circulation distribution with two parallel planes as jet boundary versus wing chord.

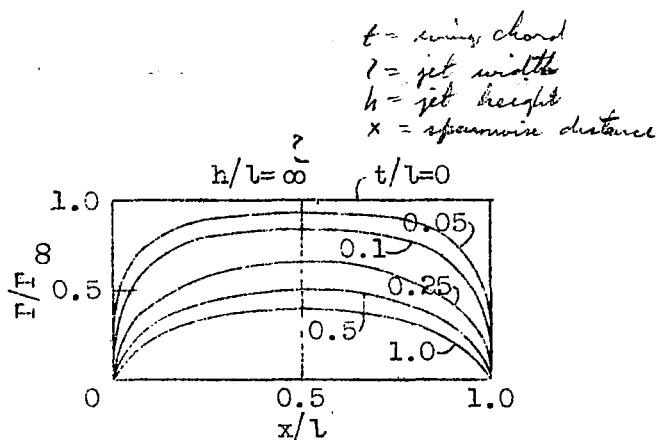


Figure 4.-Distribution of circulation with square jet section, $h/l = 1$.

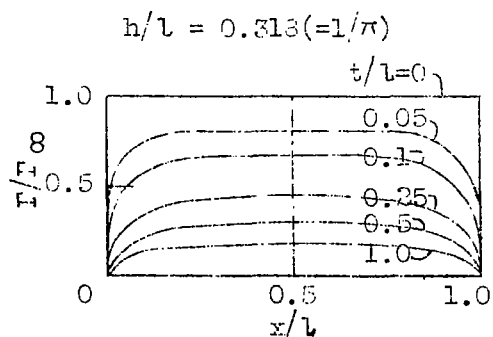


Figure 5.-Distribution of circulation with rectangular jet section, $h/l = 0.318$.

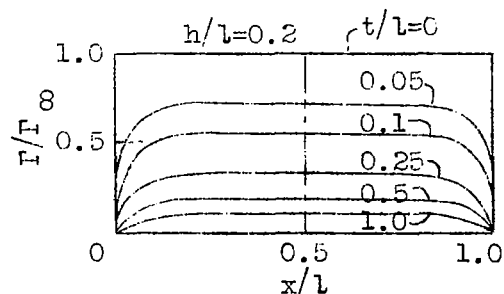


Figure 6.-Distribution of circulation with rectangular jet section, $h/l = 0.2$.

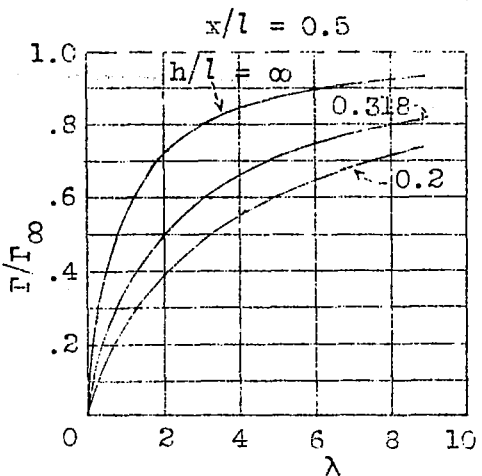


Figure 7.-Intensity of circulation in center versus λ .

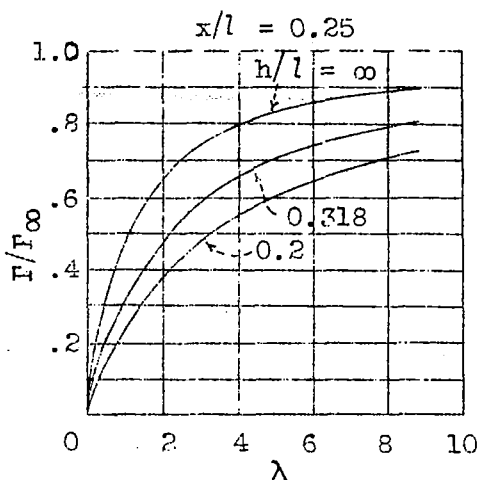


Figure 8.-Intensity of circulation with $x/l = 0.25$ versus λ .

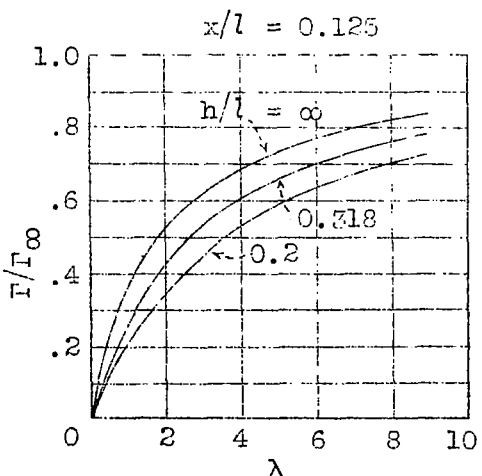


Figure 9.-Intensity of circulation with $x/l = 0.125$ versus λ .

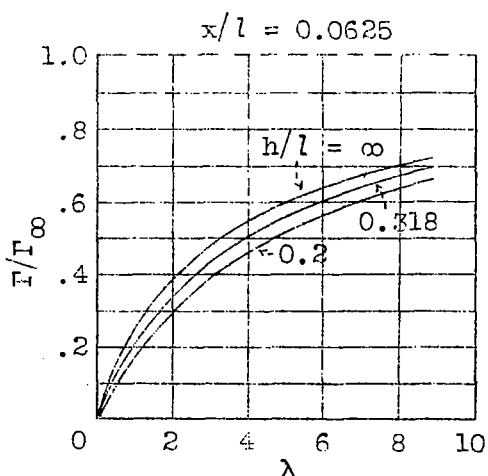


Figure 10.-Intensity of circulation with $x/l = 0.0625$ versus λ .

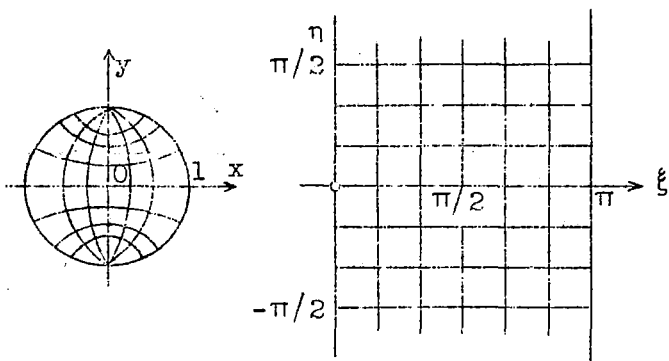


Figure 11.-Conformal transformation
of circle in a strip.

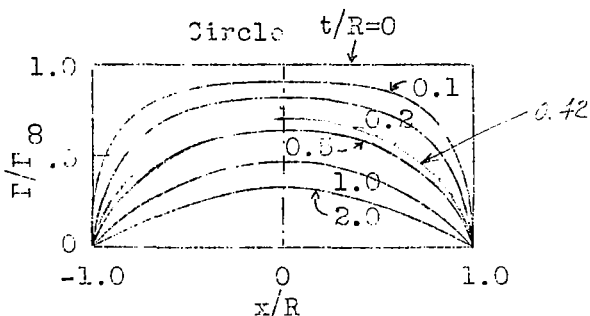


Figure 12.-Distribution of circulation with a circular
jet.

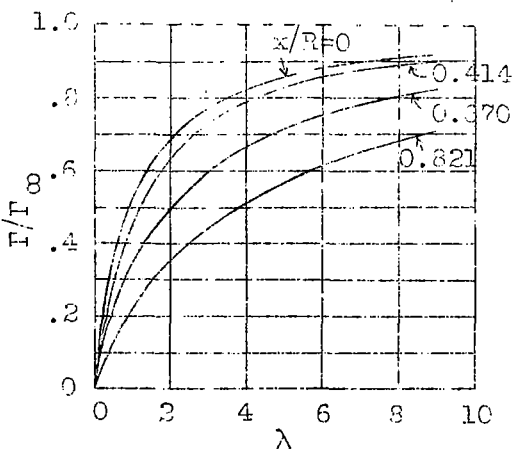


Figure 13.-
Circulation
intensity with
circular jet
versus λ .

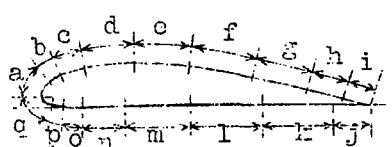
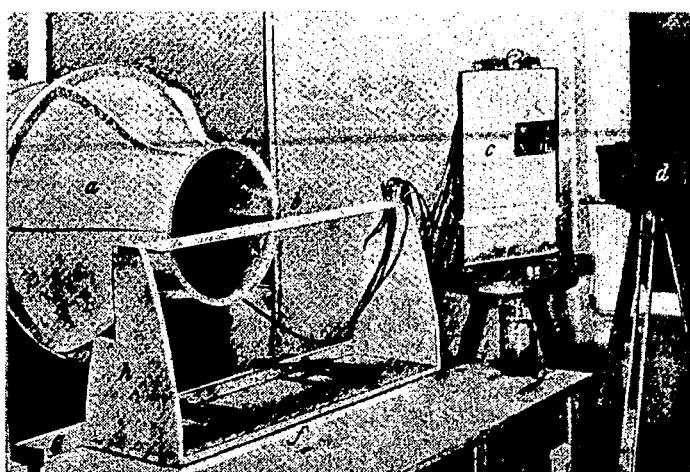


Figure 15.-Grading of
orifices across
section.

$a =$	6.0	$i =$	8.5
$b =$	4.0	$j =$	11.0
$c =$	8.0	$k =$	21.5
$d =$	15.5	$l =$	22.5
$e =$	17.0	$m =$	20.0
$f =$	20.0	$n =$	13.0
$g =$	17.0	$o =$	5.0
$h =$	12.0	$p =$	4.0
$q =$	5.5		



- a, blower nozzle
- b, airfoil model showing
test station at b.
- c, multiple pressure gauge
- d, camera
- e, scale
- g, guide rail

Figure 14.-Test arrangement

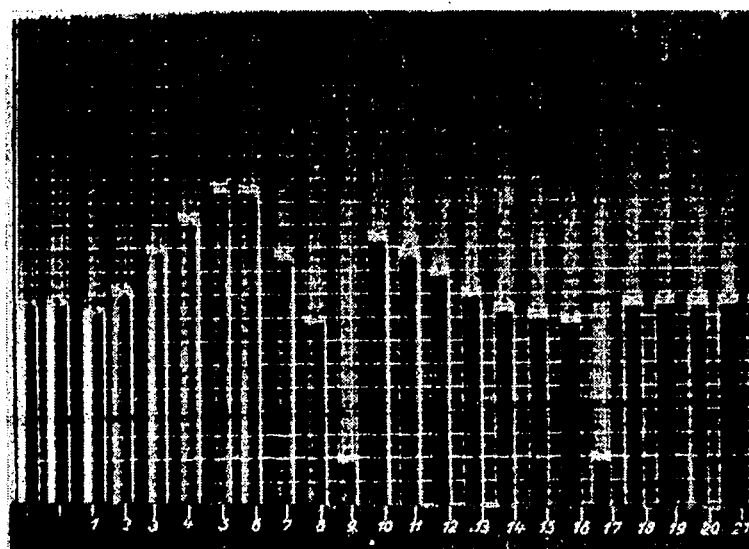


Figure 16.-Pressure distribution photograph

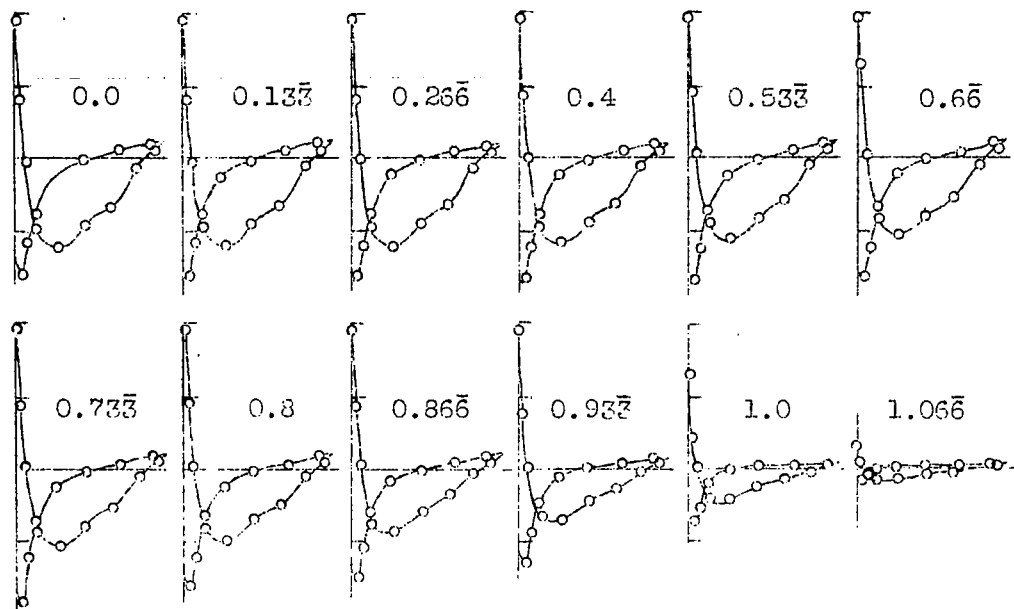


Figure 17.—Pressure profiles for square jet section, angle of attack = -3°

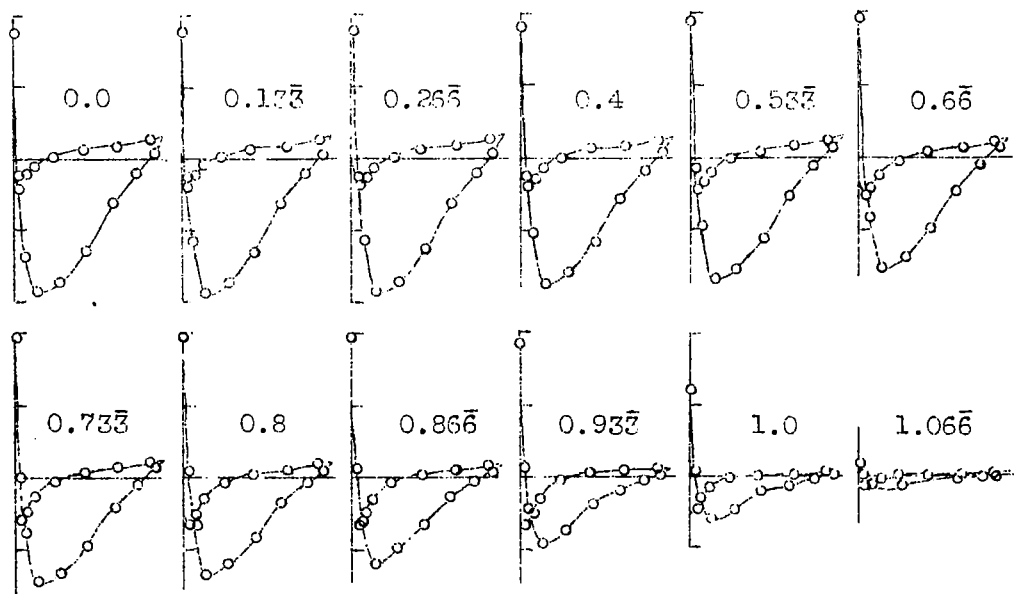


Figure 18.—Pressure profiles for square jet section, angle of attack = $+3^{\circ}$

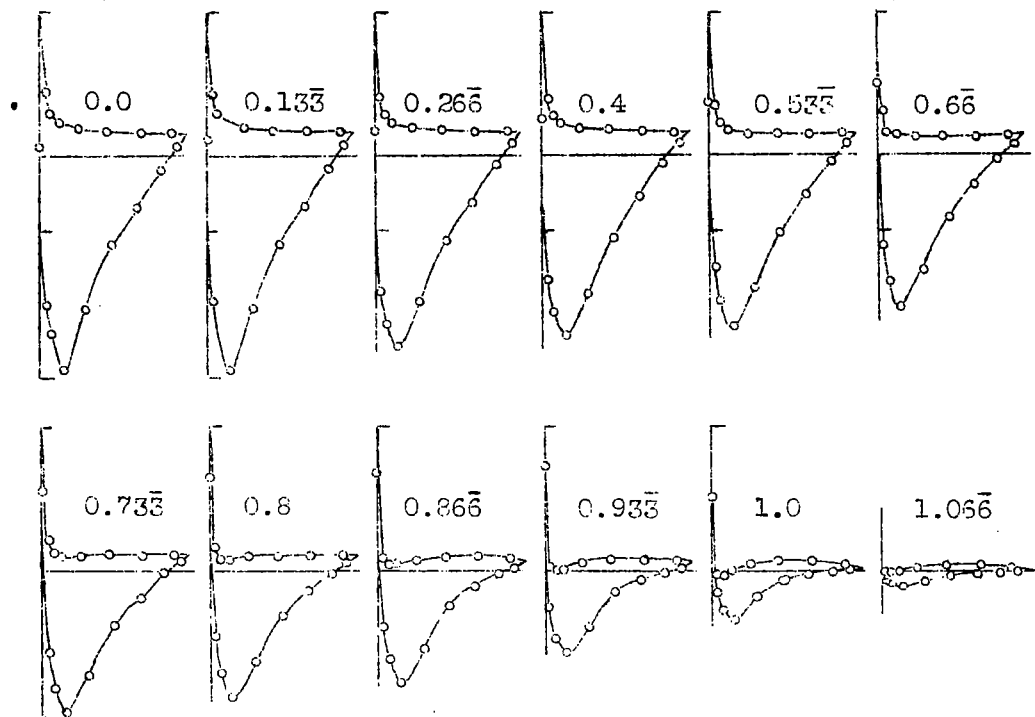


Figure 19.-Pressure profiles for square jet section, angle of attack = $+9^{\circ}$.

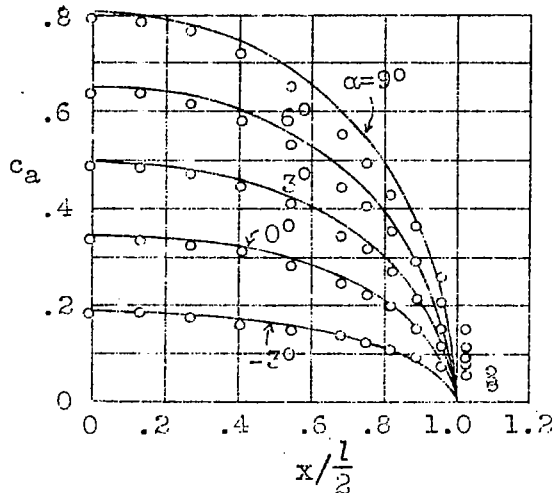


Figure 20.-
Lift distribution
with square
jet section.

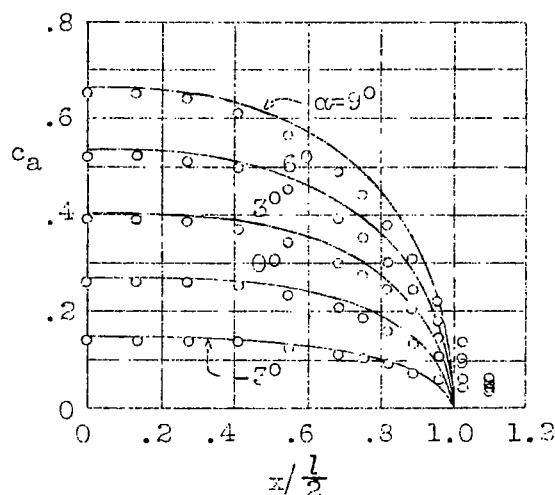


Figure 21.-
Lift distribution
with rectangular
jet section,
($h/l = 0.5$).

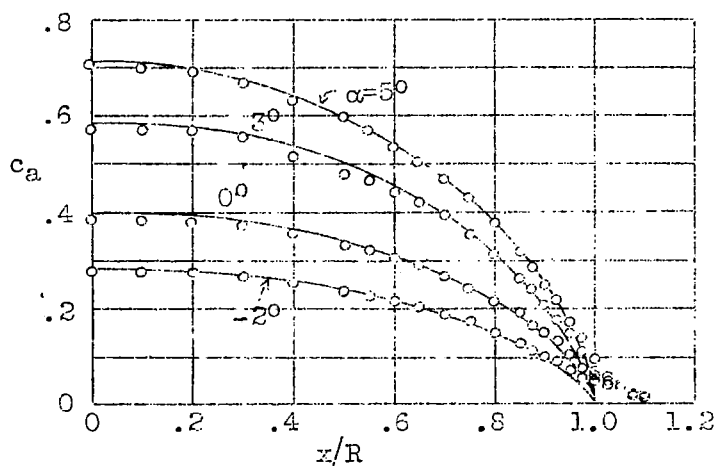


Figure 22.-
Lift distribution
with circular
jet section.

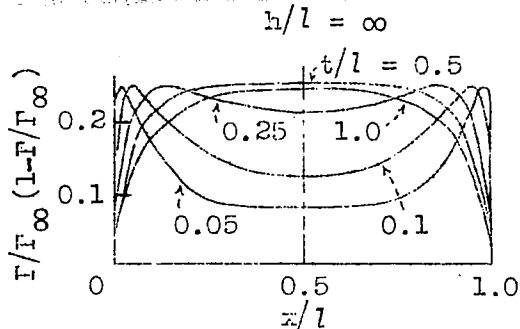


Figure 27.-Distribution of drag density with strip, ($h/l = \infty$).

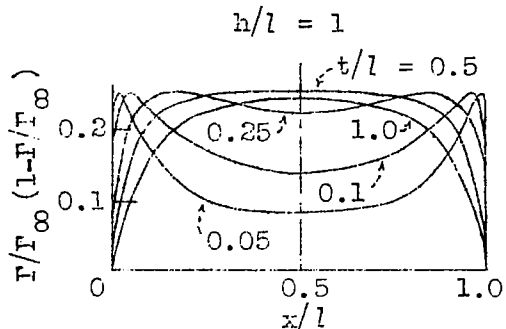


Figure 24.-Distribution of drag density with square jet section, ($h/l = 1$).

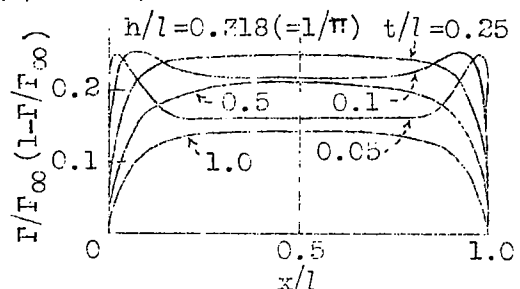


Figure 25.-Distribution of drag density with rectangular jet section, (h/l) = 0.318

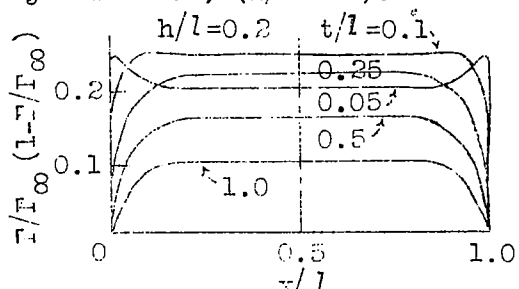


Figure 26.-Distribution of drag density with rectangular jet section, (h/l) = 0.2

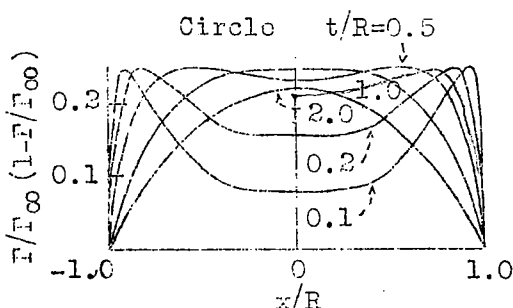


Figure 27.-Distribution of drag density with circular jet section.

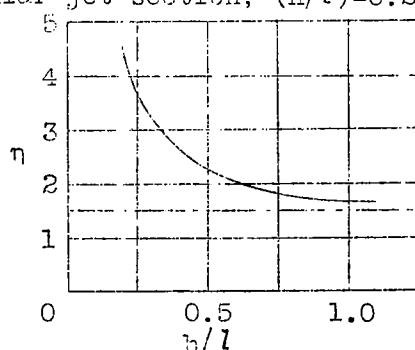


Figure 28.-Trend of drag coefficient η

NASA Technical Library



3 1176 01437 3857